AD_____

Award Number: W81XWH-10-1-1017

TITLE: Chemically Modified Bacteriophage as a Streamlined Approach to Noninvasive Breast Cancer Imaging

PRINCIPAL INVESTIGATOR: Michelle E. Farkas, Ph.D.

CONTRACTING ORGANIZATION: University of California, Berkeley
Berkeley, CA 94720

REPORT DATE: October 2011

TYPE OF REPORT: Annual Summary

PREPARED FOR: U.S. Army Medical Research and Materiel Command
Fort Detrick, Maryland 21702-5012

DISTRIBUTION STATEMENT: Approved for Public Release;
Distribution Unlimited

The views, opinions and/or findings contained in this report are those of the author(s) and should not be construed as an official Department of the Army position, policy or decision unless so designated by other documentation.

REPORT DOCUMENTATION PAGE

Form Approved
OMB No. 0704-0188

Public reporting burden for this collection of information is estimated to average 1 hour per response, including the time for reviewing instructions, searching existing data sources, gathering and maintaining the data needed, and completing and reviewing this collection of information. Send comments regarding this burden estimate or any other aspect of this collection of information, including suggestions for reducing this burden to Department of Defense, Washington Headquarters Services, Directorate for Information Operations and Reports (0704-0188), 1215 Jefferson Davis Highway, Suite 1204, Arlington, VA 22202-4302. Respondents should be aware that notwithstanding any other provision of law, no person shall be subject to any penalty for failing to comply with a collection of information if it does not display a currently valid OMB control number. **PLEASE DO NOT RETURN YOUR FORM TO THE ABOVE ADDRESS.**

1. REPORT DATE	2. REPORT TYPE	3. DATES COVERED
October 2011	Annual Summary	28 September 2010 – 27 September 2011

4. TITLE AND SUBTITLE

Chemically Modified Bacteriophage as a Streamlined Approach to Noninvasive Breast Cancer Imaging

5a. CONTRACT NUMBER

5b. GRANT NUMBER
W81XWH-10-1-1017

5c. PROGRAM ELEMENT NUMBER

6. AUTHOR(S)

Michelle E. Farkas, Ph.D.

E-Mail: mfarkas@berkeley.edu

5d. PROJECT NUMBER

5e. TASK NUMBER

5f. WORK UNIT NUMBER

7. PERFORMING ORGANIZATION NAME(S) AND ADDRESS(ES)

University of California, Berkeley
Berkeley, CA 94720

8. PERFORMING ORGANIZATION REPORT NUMBER

9. SPONSORING / MONITORING AGENCY NAME(S) AND ADDRESS(ES)
U.S. Army Medical Research and Materiel Command
Fort Detrick, Maryland 21702-5012

10. SPONSOR/MONITOR'S ACRONYM(S)

11. SPONSOR/MONITOR'S REPORT NUMBER(S)

12. DISTRIBUTION / AVAILABILITY STATEMENT
Approved for Public Release; Distribution Unlimited

13. SUPPLEMENTARY NOTES

14. ABSTRACT

While capable of visualizing tumors with high sensitivity, current diagnostic imaging methods yield little information with regard to the type of cancer present; biopsy follow-ups are required to determine prognosis and treatment. As a non-invasive alternative, we directly convert cell surface marker-specific phage isolated from library screens into imaging agents that can target and differentiate breast cancer tissues. By using efficient synthetic protocols, we are able to selectively conjugate small molecules to the phage coat proteins. The abilities of the modified phage to bind their targeted cell surface receptors following these manipulations are evaluated in vitro by using flow cytometry and confocal microscopy assays. We have confirmed that the synthetic modifications performed (installation of fluorophores and polyethylene glycol chains) do not significantly alter phage binding ability. Initial experiments in vivo with mouse xenograft models are used to determine biodistribution and tumor targeting abilities of the agents in a physiological setting.

15. SUBJECT TERMS
None provided.

16. SECURITY CLASSIFICATION OF:			17. LIMITATION OF ABSTRACT	18. NUMBER OF PAGES	19a. NAME OF RESPONSIBLE PERSON
a. REPORT	b. ABSTRACT	c. THIS PAGE			USAMRMC
U	U	U	UU	22	19b. TELEPHONE NUMBER *(include area code)*

Table of Contents

INTRODUCTION: Diagnostic imaging methods, such as positron emission tomography (PET), play a key role in the detection, treatment, and study of breast cancer. Yet while enabling disease visualization, current imaging methods yield little information with regard to the type of cancer present; biopsy follow-ups are required to determine a patient's prognosis and recommended treatment regimen. As a non-invasive alternative, my research involves the chemical modification and subsequent use of filamentous bacteriophage targeting specific breast cancer markers (HER2 and EGFR) in order to visualize and study these tumors in mice. The generation of imaging agents relies on the attachment of functional groups that can be detected (i.e. radioactive or fluorescent labels) to a molecule that shows some specificity for a marker of interest on the cell surface. The binding moieties are selected through the use of phage display techniques, where members of a library of diversified phage are isolated based on their ability to associate with a particular target. We have shown that we can selectively modify a significant portion of the pVIII coat proteins lining the sides of the phage in order to incorporate these labels and other small molecules. Following generation and modification of the targeted agents, their selectivity is evaluated *in vitro* and *in vivo*. By directly converting phage recovered from library screens into imaging agents, this research has the potential to significantly stream-line the process of targeted imaging agent generation.

BODY: My research involves the use of chemically modified filamentous (fd) bacteriophage in the targeting and differentiation of breast cancer tissues bearing specific surface markers, directly converting library-identified phage into imaging agents. In the first year of the fellowship, I have generated and modified HER2 and EGFR-targeting phage to display small molecules, and performed *in vitro* evaluations of the phage‟s abilities to bind breast cancer and other cell lines that express the targeted markers of interest at varying levels. Xenograft models of breast cancer have been prepared in order to perform preliminary optical imaging experiments to evaluate phage tumor targeting capabilities.

Task 1. Generation and *in-vitro* evaluation of PET imaging agents based on filamentous phage

1a. Generate fd phage modified with PEG, fluorophores, and ^{18}F

The generation of diagnostic imaging agents relies on the attachment of traceable functional groups to a biomolecule that shows specificity for a cellular marker of interest. Based on moieties displayed on their terminal pIII capsid proteins, other groups have previously demonstrated the localization of phage *in vivo* to the prostate and prostate carcinoma,[1,2] and other targets.[3,4] In our research, we use filamentous bacteriophage (fd) that display marker-specific single-chain variable fragment (scFv) molecules identified by our collaborators in the laboratory of James D. Marks, M.D., Ph.D. (UCSF) using molecular evolution techniques (**Figure 1**). Phage targeting a variety of markers have been isolated in their laboratory. In the studies described in this report, I have used fd that are selective for the epidermal growth factor receptor (EGFR)[5], and human epidermal growth factor Receptor 2 (HER2 or ERBB-2).[6] Phage targeting botulinum toxin serotype A (BoNT/A)[7] have been used as a control. Phage targeting HER3 (whose overexpression has been shown to be a marker of reduced patient breast cancer-specific survival[8]), CD44 (a cell adhesion molecule involved in tumor metastasis, which is also a cell surface marker used to identify human cancer stem cells[9,10]), and CD73 (a cell surface protein overexpressed in many solid tumors, which may promote tumor progression[11,12]) are currently in the process of being generated, in order to be similarly modified and evaluated *in vitro* and *in vivo*.

Anti-EGFR, -HER2, and –BoNT/A phage-infected *Escherichia coli* (*E. coli)* had been previously given to the Francis lab in order further propagate fd of interest for our studies, along with methodology to do so.[13] In my hands, a number of the steps required further optimization, including scales and temperatures at various stages in the process. Furthermore, it was determined that after ~30 days individual *E. coli* colonies would continue to grow when cultured, but produced diminishing yields of phage and in some cases, none at all. The reason for this has not been investigated. Recovery was dependent upon phage type and time elapsed following re-plating of *E. coli* colonies. Phage targeting EGFR, HER2, and BoNT/A were each produced several times

for further modification and experiments. The optimized procedure for phage production is described in the *methods* section of this report.

In order to append small molecules to phage pVIII coat proteins, I have used a reaction developed by the Francis group to site-selectively convert N-terminal alanines into ketone groups.[14-16] By exposing phage to 30-100 mM pyridoxal 5‟-phosphate (PLP) at pH 6.5 for 13 hours, it had been shown that over 80% of the approximately 4500 pVIII coat proteins can be modified. These groups can then be reacted further with alkoxyamines in order to display small molecules or polyethylene glycol (PEG) chains via oxime formation (Figure 1).[17-18] Phage were modified with alexafluor-488 (AF-488) and alexafluor-647 (AF-647) alkoxyamines for *in vitro* and *in vivo* studies. While AF-488 had been previously conjugated to phage, fairly low levels of modification had been obtained. Reaction conditions were optimized in order to increase levels of dye incorporation. In this endeavor, a significant number of methods tested resulted in the abolishment of phage binding to cell lines over-expressing the targeted receptor, likely due to mis-folding of the scFv subunit. Final protocols resulted in approximately 7-8% modification of pVIII proteins, and phage retained cell binding capabilities. AF-647 conjugated phage were used for *in vivo* optical imaging experiments on account of the dye‟s improved tissue penetration ability versus AF-488. Reacting AF-647 with PLP-modified phage under conditions optimized for AF-488 resulted in extremely low levels of modification (< 0.5%). Further optimization of the conjugation reaction resulted in higher levels of incorporation of AF-647 (~8%). Using the same conditions with AF-488 yielded even more incorporation (> 30%) however these phage suffered from significantly diminished solubilities and could only be used at low concentrations. Conditions used for the PLP transamination and subsequent reactions are described in detail in the *methods* section.

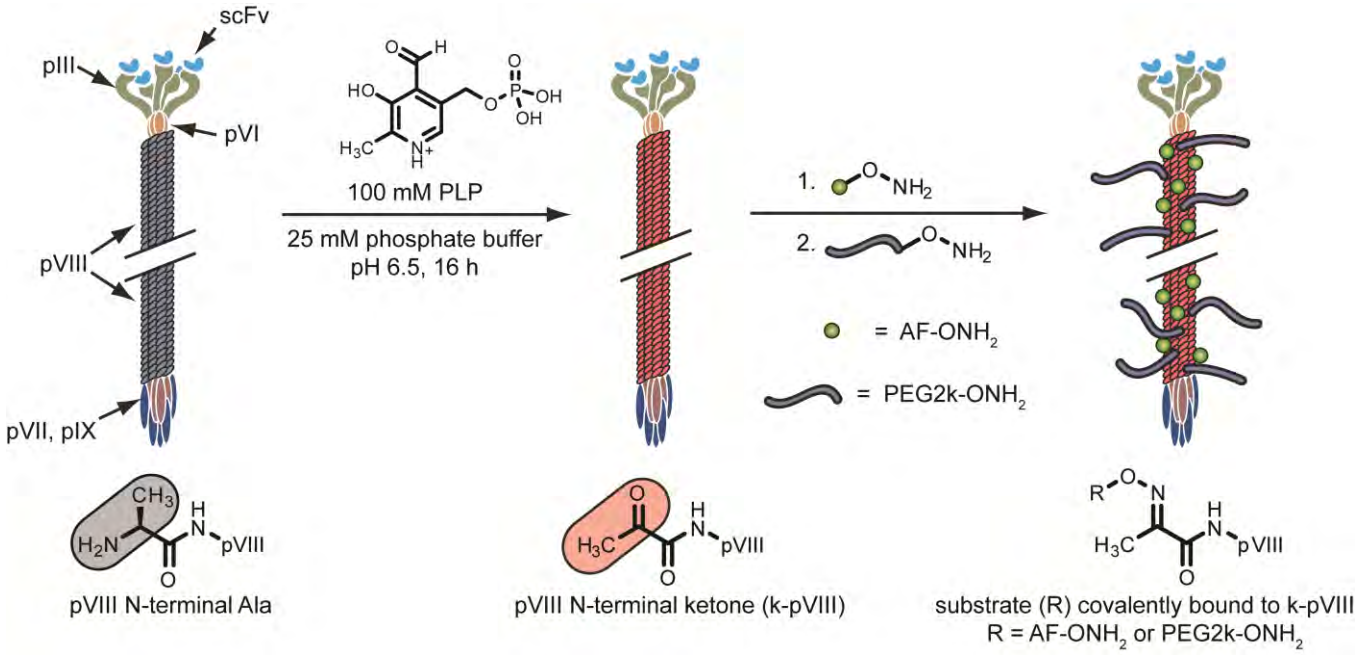

Figure 1. Chemical modification of filamentous (fd) phage. N-terminal alanines (Ala) of the pVIII coat proteins lining the filamentous phage are converted to ketone groups, which can be subsequently modified with small molecule alkoxyamines including dyes (AF-ONH_2) and polyethylene glycol chains (PEG2k-ONH_2).

Previous work in our group has shown that various numbers of PEG chains can be introduced per phage, ranging from 20-70% (900-3150 copies per phage). A reverse-phase HPLC method has been developed to accurately determine the ratio of modified to unmodified capsid proteins.[18] Zeta potential measurements have shown that increased numbers of 5 kDa PEG chains shield surface charge,[19] potentially improving phage circulation properties. Following modification with AF-647, 5 kDa PEG-alkoxyamine was reacted with anti-

EGFR phage. PEG-AF-647-anti-EGFR phage were generated with varying levels of PEG (10%, 25%, 50%, and 75%). The resulting phage were evaluated with regard to cell binding and *in vivo*, both discussed later in this report.

At the time of proposal submission, preliminary studies involving the labeling of fd with ^{18}F had been performed via the oxidative coupling of ^{18}F-fluoroaniline to small molecule alkoxyamines containing aminophenol groups. Further work involving phage radiolabeling is still in progress.

1b. Evaluation of phage binding selectivity in serum and cell culture

Presumably, the biomarker binding site at the phage terminus is located a few nanometers from the bulk of the chemical modifications, thereby minimizing interference with scFv binding (**Figure 1**). In preliminary studies testing the potential for interference, anti-EGFR fd were minimally functionalized with AF-488 fluorescent dye molecules and varying numbers of 5 kDa PEG chains. Using flow cytometry, these samples were evaluated for their ability to bind MDA-MB231 cells (EGFR-positive), and compared to control phage (anti-BoNT/A), which do not bind EGFR. Excellent binding selectivity was observed at all levels of PEG modification, although increased levels of PEG resulted in slightly diminished binding. Furthermore, neither anti-EGFR nor anti-BoNT/A phage recognized SUM-52PE cells, which lack the targeted receptor (data not shown).[18]

Following reactions yielding increased levels of AF-488 modification, anti-EGFR, anti-HER2, and anti-BoNT/A phage binding were evaluated via flow cytometry in a panel of receptor positive and negative cell lines. These cell lines included both basal and luminal sub-type immortalized breast cancer cells of a variety of origins (HCC1954, M6 (mouse), M6c (mouse), MCF-7, MCF-7 clone 18, MDA-MB-231, MDA-MB-453, SKBR3, SUM52-PE – all human unless otherwise noted), and non-breast cancer cells (U87MG (glioblastoma/astrocytoma), A431 (epidermoid carcinoma), Jurkat (T-cell leukemia), L3.6pl (pancreatic carcinoma)). Representative data from flow cytometry experiments in MDA-MB-231 (basal, adenocarcinoma), MCF-7 clone 18 (a HER2-overexpressing variant of the luminal, adenocarcinoma cell line MCF-7), MDA-MB-453 (luminal, metastatic carcinoma), and HCC1954 (basal, ductal carcinoma) breast cancer cell lines are shown in **Figure 2**, and a compilation of the results from all experiments is shown in **Table 1**. Independent of PEG modification levels, little or no non-specific binding was observed in these assays. Procedures are described in the *methods* section, and forward- and side-scatter plots are in the *supporting information* section at the conclusion of this report. Experiments to detect non-specific phage binding in serum (rat, rabbit, or mouse) have not yet been conducted.

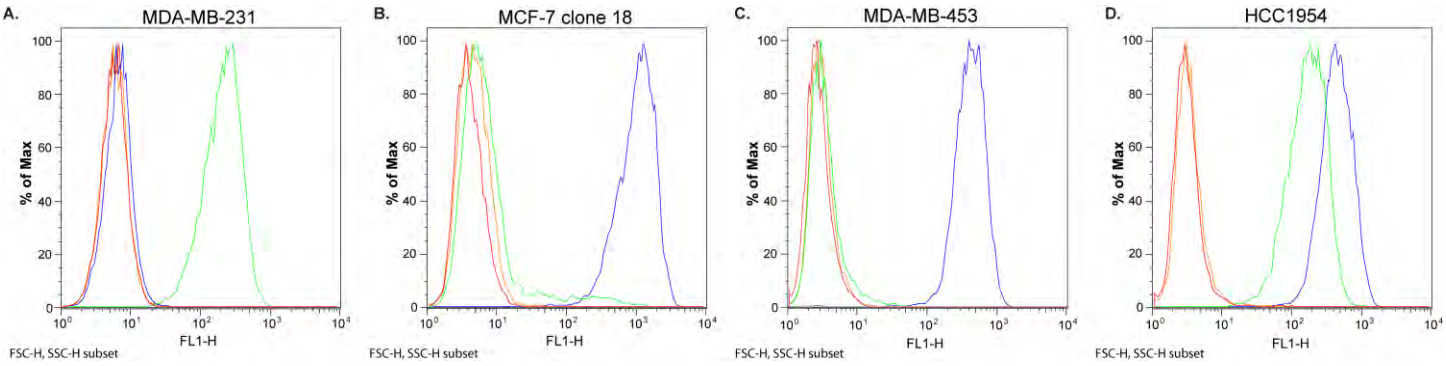

Figure 2. Representative flow cytometry data from phage binding experiments. Histograms are shown for (**a**) MDA-MB-231, (**b**) MCF-7 clone 18, (**c**) MDA-MB-453, and (**d**) HCC1954 cells treated with anti-EGFR (green), anti-HER2 (blue), and anti-BoNT/A (orange) phage. Untreated cells are shown in red. Forward and side scatter data for these plots are shown in *supporting information*.

cell line	cancer type	subtype	HER2/EGFR	anti-EGFR	anti-HER2	anti-BoNT/A
MDA-MB-231	breast, adenocarcinoma	basal	-/+	√	x	x
SKBR3	breast, adenocarcinoma	luminal	+/+	√	√	x
L3.6pl	pancreatic, carcinoma	N/A	+/+	√	√	x
MCF-7	breast, adenocarcinoma	luminal	-/-	x	n.d.	x
MCF-7 clone 18	MCF-7 variant	luminal	+/-	x	√	x
SUM52-PE	breast, carcinoma	luminal	+/-	x	n.d.	x
Jurkat	t-cell leukemia	N/A	-/-	x	x	x
M6	mouse, breast	N/A	-/+	√	n.d.	x
M6c	mouse, breast metastasis	N/A	-/+	√	n.d.	x
MDA-MB-453	breast, metastatic carcinoma	luminal	+/-	x	√	x
HCC1954	breast, basal ductal carcinoma	basal	+/+	√	√	x
A431	epidermoid carcinoma	N/A	-/+	√	x	x
U87MG	neuronal glioblastoma	N/A	-/+	√	x	x

Table 1. Cell line characteristics and phage binding. Each cell line used for phage binding experiments is shown, accompanied by the cancer type, subtype (for breast cancer cell lines), established HER2 and EGFR expression, and binding of the anti-EGFR, -HER2, and -BoNT/A phage, respectively. Plus and minus signs indicate the presence and absence of the marker in a given cell line. Green check marks indicate phage binding to the cell line, while red crosses indicate no binding. N/A = not applicable and n.d. = not determined (these experiments are pending).

Cell-based flow cytometry analyses were subsequently used as „quality-control" in order to assess the abilities of phage to bind targeted cells following various chemical modifications and reaction optimizations, and prior to use in any *in vivo* assays. Additionally, a live-cell confocal microscopy experimental protocol was devised in order to visualize phage cell binding and uptake. Experiments were performed using the selected breast cancer cell lines HCC1954, MDA-MB-231, and MCF-7 clone 18. Anti-EGFR and anti-HER2 phage were labeled with AF-488 and AF-647, respectively. MDA-MB-231 (HER2 negative, EGFR positive) and MCF-7 clone 18 (HER2 positive, EGFR negative) cells were both individually treated with each type of phage and co-cultured and treated with both types of phage concurrently. In the case of HCC1954, which overexpresses both HER2 and EGFR, cells were both separately and simultaneously treated with each phage type (**Figure 3, Figures S5-S10**). Following prolonged phage exposure to cells, uptake was observed in some instances. Further microscopy experiments to evaluate cellular uptake of phage and the mechanism by which it occurs are in progress. Protocols used in the assay are described in the *methods* section.

Task 2. *In vivo* animal imaging with ^{18}F agents

2a. Determination of phage distribution in healthy animals

The evaluation of phage bio-distribution in healthy animals has been postponed pending the completion of initial optical imaging experiments using tumor bearing mice and optimization of the chemistry to modify the agents with ^{18}F.

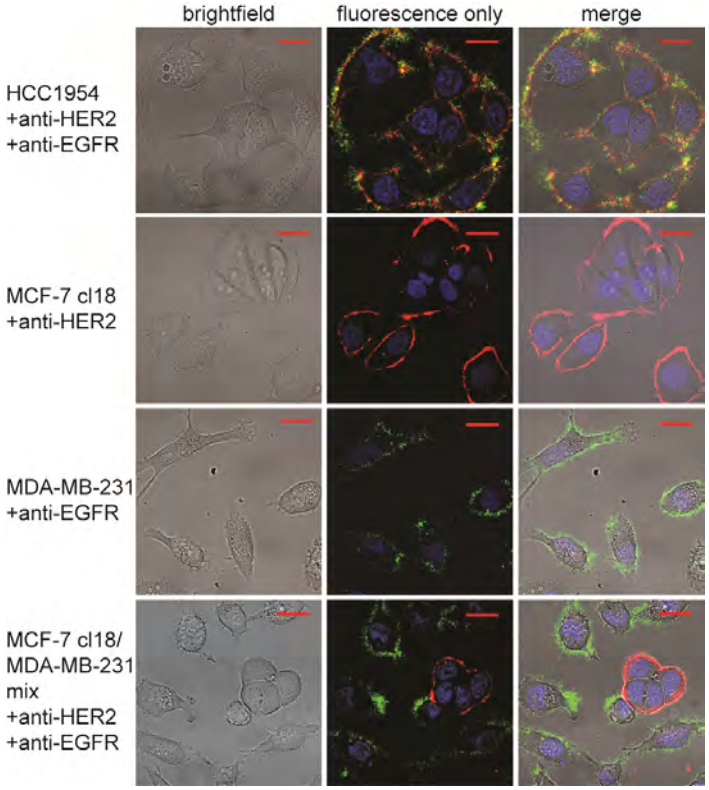

Figure 3. Live-cell confocal microscopy of phage binding to cell surface markers. Anti-HER2 (red) and anti-EGFR (green) phage binding to HCC1954, MCF-7 clone 18, MDA-MB-231, and co-cultured MCF-7 clone 18 and MDA-MB-231 cells are shown; cell lines and phage added are indicated along each row. Nuclei are stained with DAPI (blue). Scale bars indicate 20 μm. Control samples and individual channels are shown in supporting information.

2b. Establishment and imaging of xenograft tumors using optical imaging and PET in mice.

Initial animal experiments have been carried out using fluorophore labeled anti-EGFR, anti-HER2, and anti-BoNT/A phage with a fluorescence molecular tomography optical imaging system. By using the optical imaging modality, results from *in vitro* cell culture binding experiments can be directly correlated with *in vivo* targeting experiments, as identical agents are used for both assays. Two distinct preliminary animal imaging experiments have been performed. In one, HCC1954 cells were subcutaneously implanted in the hind flank of nude SCID mice, which were subsequently injected and imaged with HER2-targeting phage modified with AF-647 via the tail vein (**Figure 4**). The agents did not appear to be taken up by the tumor; major sites where the phage accumulated were the liver and kidneys, followed by excretion via the bladder. At increased contrast levels, it appears that they may also be localizing in the inguinal lymph nodes at earlier time points (4-8 h; not shown, and in the tumors at later time points (48 h; not shown). For the most part, agents were found to clear 72 hours after injection. Following imaging at the final time point(s) animals were sacrificed, and *ex-vivo* bio-distribution was performed (not shown). Additional sites of agent accumulation included the spleen, and to varying degrees, the pancreas, lungs, and tumor. A number of potential issues occurred with this experiment. The viability of the tumors was unknown – they did not seem to be necrotic, but were already of a larger size (>0.5 cm) than we had originally planned for imaging. Despite the appearances of the tumors as solid masses, during the course of *ex-vivo* analyses, the tumors were found to contain significant amounts of clear liquid, which we believe may have been the result of cysts. Further experimental details can be found in the methods section.

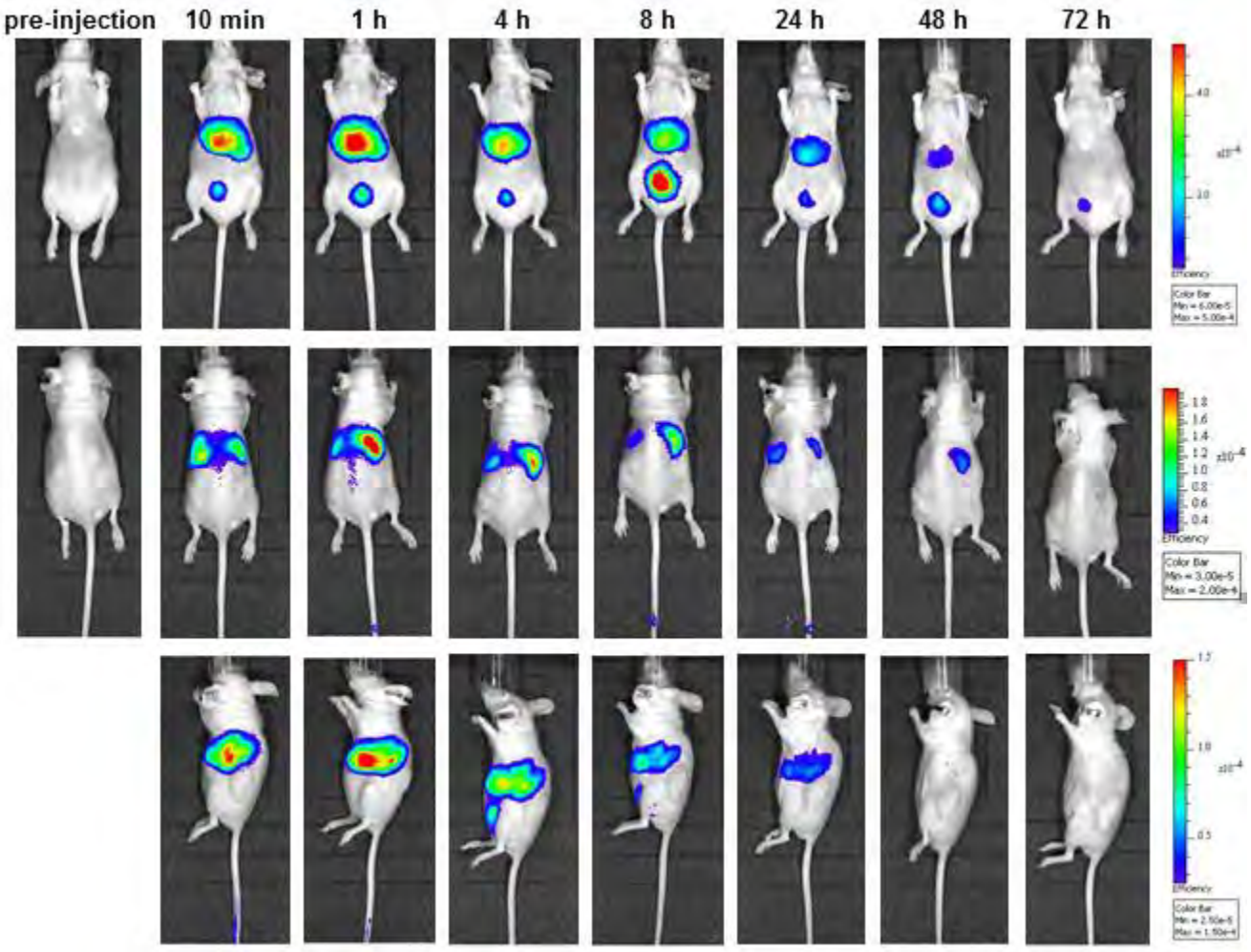

Figure 4. Imaging of mice implanted with HCC1954 human breast cancer cells. Representative images for mice injected with anti-HER2 phage via the tail vein in the supine, prone, and side positions over the course of 72 h. In the supine images, the agent is primarily observed in the liver and bladder, while in the prone position, the kidneys are also observed. All images were acquired from a single mouse injected with anti-HER2 phage, and normalized to the same scale. No pre-injection image was taken from the side perspective in this experiment.

In another experiment, MDA-MB-231 cells were orthotopically implanted into the number four mammary fat pads. On opposite sides, two separate implantations were made: the left side received MDA-MB-231 cells stably transfected with a luciferase reporter gene, while right side received the parental MDA-MB-231 cell line. Luminescence imaging with luciferin was used to ensure the viability of the xenograft cells (not shown). Mice were imaged with anti-EGFR (**Figure 5**) and anti-BoNT/A phage (data not shown) without PEG modification. All phage were given via tail-vein injections. The two phage types had similar localization profiles across the course of imaging. As with the HCC1954 xenografts and anti-HER2 phage, the major sites of accumulation were the liver and kidneys, and signal to the bladder increased over time. With these tumors, it is apparent (even without changing the contrast) that there is accumulation in the area of the tumor/inguinal lymph nodes. However, due to the location of the mammary fat pad, it is difficult to distinguish tumor from lymph node position, and in the supine position, signal from the liver and bladder is too strong to visualize the area at higher contrast levels without significant signal bleed from those sites. The majority of the agents were found to clear after 48 h. *Ex vivo* biodistribution was performed following sacrifice at the terminal time points, and revealed that in addition to the liver and kidneys, additional agent accumulation occurred in the spleen and tumor derived from the parental MDA-MB-231 cell line. However, no agent was found in the transfected cell line. We have received the reporter MDA-MB-231 cell line in our laboratory and cell binding experiments with the phage will be performed. There was little difference between the targeted (anti-EGFR) and un-targeted (anti-BoNT/A) phage.

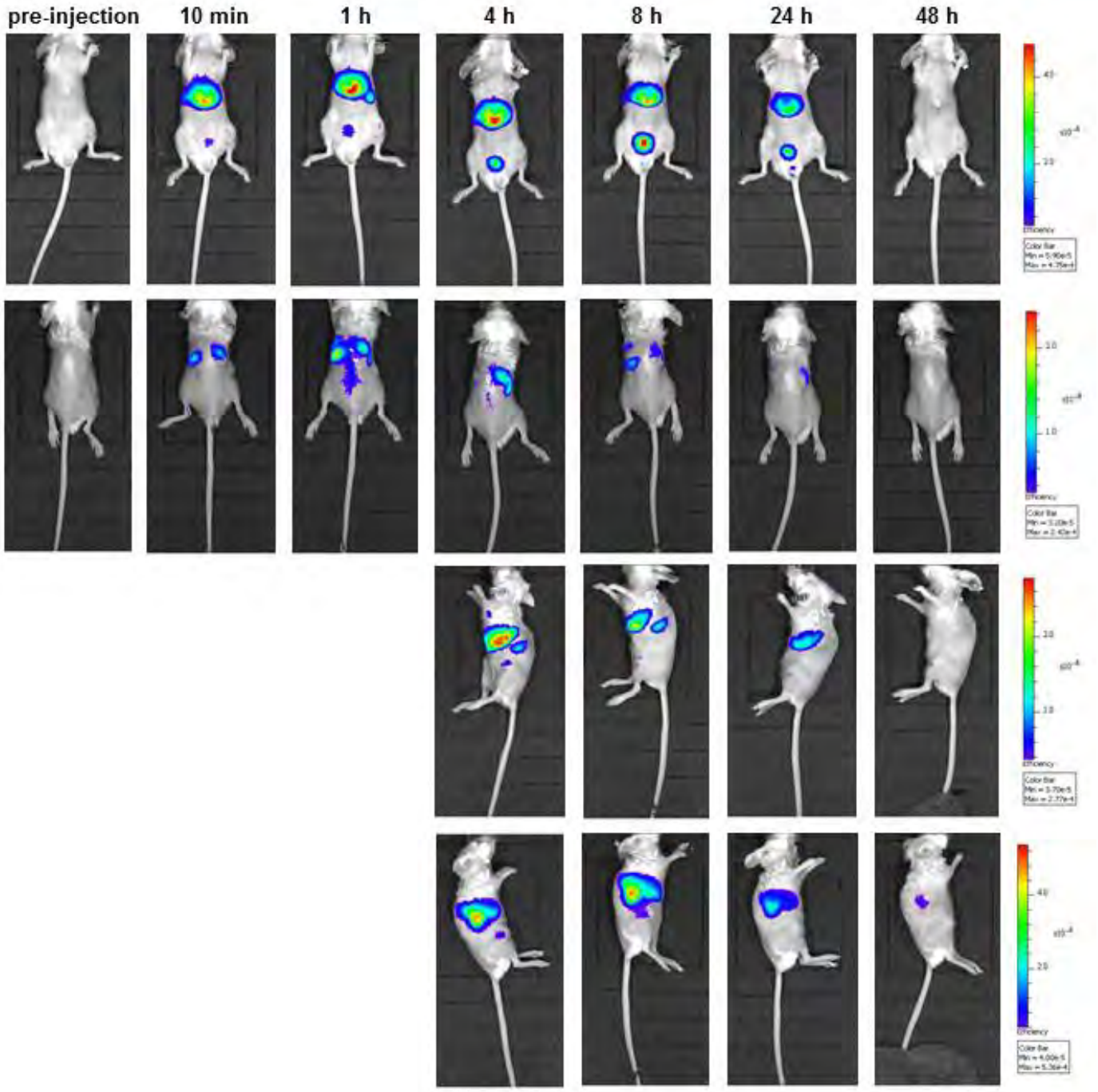

Figure 5. **Imaging of mice orthotopically implanted with MDA-MB-231 cells.** Representative images for mice injected with anti-EGFR phage via the tail vein in the supine, prone, and side positions over the course of 48 h are shown. In the supine images, the agent is primarily observed in the liver and bladder, while in the prone position the kidneys are also observed. In both the left side (where the cell line transfected with the luciferase reporter gene has been implanted) and the right side (where the parental cell line has been implanted), it is difficult to distinguish sites where the tumors are located from potential inguinal lymph node positions, however, no agent is observed in those locations after 8 h. All images were acquired from a single mouse injected with anti-EGFR phage, and normalized to the same scale. No images were generated from the side perspectives prior to the 4 h time-point in this experiment.

In an effort to improve agent circulation time and biodistribution, anti-EGFR phage with 25% (**Figure 6**) and 75% (data not shown) of the pVIII coat proteins modified with PEG was also used for imaging. Description of the modification of phage with PEG is described further above (*Task **1a***). Comparing the images in **Figures 5** and **6**, it is likely that the addition of PEG chains results in an extension of circulation time, as evidenced by the amount of time taken for maximum amount of signal to reach the liver (1 h for 0% PEG, 3 h (time point not shown) for 25% PEG). No control (anti-BoNT/A) phage bearing PEG chains were used in this

experiment. Accumulation is again primarily observed in the liver, bladder, and kidneys, and it is difficult to distinguish the tumors from lymph node sites *in vivo*. Increasing the level of PEG modification to 75% did not appear to result in a significant change, however, as both PEGylated phage were only used in a single pilot experiment each, we do not believe these results to be conclusive. In future studies, I plan to further assess the tumor binding ability and circulation/biodistribution of the PEG-modified phage. An appropriate xenograft model for less ambiguous visualization of agent binding *in vivo* is currently being explored.

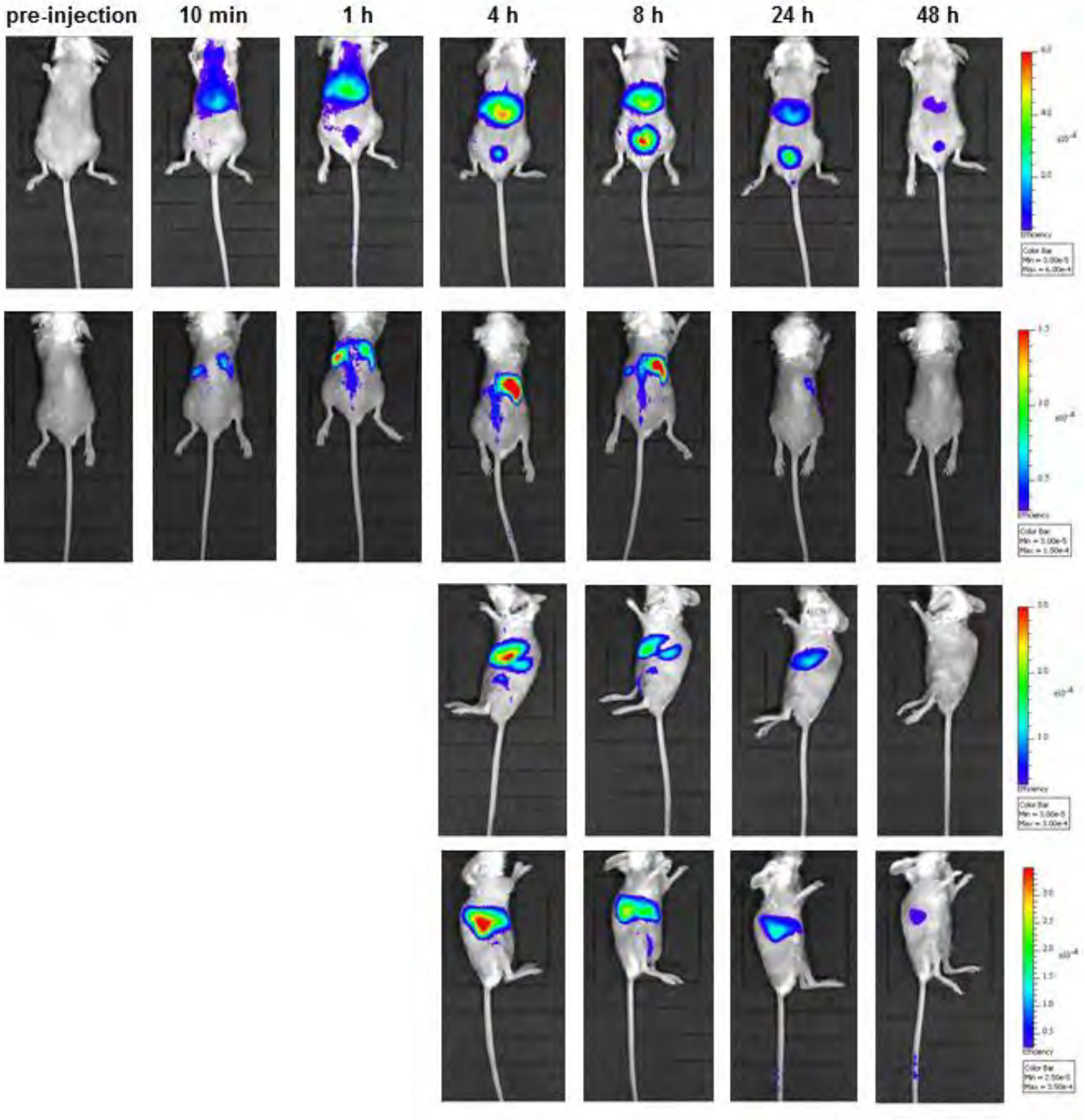

Figure 6. Imaging of mice orthotopically implanted with MDA-MB-231 cells. Representative images for mice injected with anti-EGFR phage possessing PEG modifications via the tail vein in the supine, prone, and side positions over the course of 48 h are shown. In the supine images, the agent is primarily observed in the liver and bladder, while in the prone position the kidneys are also observed. In both the left side (where the cell line transfected with the luciferase reporter gene has been implanted) and the right side (where the parental cell line has been implanted), it is difficult to distinguish sites where the tumors are located from potential inguinal lymph node positions. All images were acquired from a single mouse injected with anti-EGFR phage, and normalized to the same scale. No images were generated from the side perspectives prior to the 4 h time-point in this experiment.

Methods:

1. Phage propagation from infected *E. coli.* All phage described herein (anti-EGFR, anti-HER2, anti-BoNT/A) were generated and purified using identical conditions. A single colony of *E. coli* TG1 cells infected with fd phage are inoculated into 5 mL of LB media containing 15 μg/mL tetracycline (a tetracycline-resistance gene was previously introduced into the genome), followed by incubation with shaking at 37 °C and 250 rpm. After approximately 9 h of growth, the starter culture was split in half -- 2.5 mL of the culture was added to 1 L of 2xYT media. The culture was incubated at 30 °C for 16-18 h at 250 rpm. The media was recombined and the cells were removed via centrifugation at 6,000 rpm for 20 min at 4 °C. The supernatant was collected and fd phage were precipitated for 1 h at 4 °C (on ice) after addition of and thorough mixing with 1/10 volumes of 20% PEG8k/2.5M NaCl solution (200 mL for 2 L media). The resulting suspension was centrifuged at 8,000 rpm for 30 min at 4 °C, and the recovered pellet(s) were resuspended in a total volume of 35 mL PBS. The resulting phage solution was centrifuged at 6,000 rpm for 20 min at 4 °C to remove additional cellular debris. The supernatant was collected, and fd were precipitated for 1 h at 4 °C (on ice) after addition of and thorough mixing with 1/10 volume 20% PEG8k/2.5M NaCl solution. The samples were centrifuged at 9,000 rpm for 30 min at 4 °C to isolate the phage. The resulting pellet was resuspended in 3-9 mL of 4 °C PBS and stored at 4 °C.

2. PLP-mediated transamination. Fd phage were transaminated using 100 mM PLP in 100 mM phosphate buffer at r.t., pH 6.5 for ~16 h. As a result of the large excess of PLP used, phage concentrations were not found to be critical, but were typically 25-150 nM. In order to prepare the PLP solution, a sufficient volume of 250 mM phosphate buffer, pH 6.5 is added to solid PLP to make a 2 M solution (0.53 g in 1 mL). The pH is adjusted to 6.5 using 3 M NaOH (~0.5 mL), and 250 mM phosphate buffer, pH 6.5 is added to give a 1 M PLP solution. This solution must be made freshly before each use – do not freeze or store. The total reaction volume is 10 mL: 3 mL phage, 5 mL NANOpure water, 1 mL 250 mM phosphate buffer, pH 6.5, and 1 mL 1 M PLP solution generated as above. The reaction is allowed to proceed for 16-18 h at r.t. The phage are precipitated for 1 h at 4 °C after thorough mixing with 1 mL (1/10 volume) 20% PEG8k and 2.5 M NaCl, followed by centrifugation at 8,000 rpm for 30 min. The pellet is resuspended in 10 mL PBS, and the precipitation and centrifugation steps repeated. The pellet is then resuspended in 1 mL PBS, concentration determined by UV-vis, and precipitated and centrifuged; a final resuspension in PBS is performed to bring phage concentration to 250-400 nM. Phage are stored at 4 °C.

3. Fluorophore labeling. Modification of the phage with AF-488 dye is performed using the following reagent concentrations: 185 nM phage, 20 mM phosphate buffer, pH 6.2, 10 mM aniline, and 1 mM AF-488-ONH_2, PBS (to bring the reaction mixture to the correct volume; reactions are typically carried out on a 50 or 100 μL scale). The phage, phosphate buffer, and PBS are added and mixed thoroughly. The dye is then added, followed by aniline, with thorough mixing accompanied by each addition. The reaction is allowed to proceed in the dark at r.t. for 16-18 h. Following reaction, the solution is diluted to 1 mL, and the same method for precipitation and centrifugation is used as in the PLP modification. Phage are precipitated/centrifuged/re-suspended twice; the final re-suspension is in a volume of PBS to give ~200 – 300 nM phage. Phage concentrations and levels of fluorophore modification are determined by UV-vis. For higher levels of phage modification and modification using AF-647, all steps are identical; however, 100 mM (neat) aniline is used as opposed to 10 mM.

4. PEG labeling. Fluorophore labeled phage were reacted with PEG2k-ONH_2 using the following reaction conditions: 40 nM phage, 20 mM PEG2k-ONH_2, 20 mM phosphate buffer, pH 6.2, 10 mM aniline. Phage concentrations up to 200 nM were successfully used, and reactions were typically carried out on 100 μL scales. Reactions were allowed to proceed for 30 min, 1.5 h, 4 h, and 24 h, at r.t., in order to obtain modification levels of 10%, 25%, 50%, and 75%, respectively. The solutions were subsequently passed through an Illustra Nap-5 gel filtration column, and then concentrated using 100k Amicon Ultra Spin Concentrators (Millipore). The extent of PEG labeling was quantified by reverse phase HPLC (Agilent 1100 Series HPLC system using Agilent Zorbax 300 SB-CN column; solvents: A: water with 0.1% trifluoroacetic acid, B: acetonitrile with 0.1% trifluoroacetic acid). The following method was used: 35% A for 4 min; increase to 70% A at 20 min; increase to 95% A at 20.5 min; remain at 95% A until 26 min.

5. Flow cytometry binding assay. All cells were maintained using ATCC recommended guidelines. Cells were washed with PBS, trypsinized, and following quench with FBS-containing media, harvested from T75 or T175 flasks. Cells were centrifuged at 125 rcf for 5 min, and resuspended in media. Following counting via hemocytometer, the cells were centrifuged again, and resuspended in cold flow cytometry buffer (1% FBS in DPBS) at 5 million cells/mL. The cells were aliquotted into eppendorf tubes at 100 µL (500,000 cells) per tube and kept on ice. 100 µL of 0.8 nM phage in flow cytometry buffer is added to each sample (100 µL PBS is added to „untreated" samples), and are incubated for 1 h on ice in the dark. After 1 h, each sample is diluted to 1 mL with flow cytometry buffer, and the tubes are centrifuged at 2000 rpm for 5 min. The supernatant is removed, and cells are resuspended in 1 mL flow cytometry buffer, followed by centrifugation, and removal of the supernatant. The cells are finally resuspended in 200 µL flow cytometery buffer, and transferred to flow cytometry tubes. Flow cytometry experiments were performed on a FACSCalibur flow cytometer (BD Biosciences, USA) equipped with 448 nm and 633 nm lasers.

6. Live cell confocal microscopy imaging. All cells were maintained using ATCC recommended guidelines. Cells were harvested as above. Following counting via hemocytometer, cells were resuspended in normal growth media at a concentration of 25,000 cells/mL; 2 mL was added to each 35 mm glass bottom dish (MatTek Corp.). For MCF-7 clone 18/MDA-MB-231 co-cultures, 1 mL (25,000 cells/mL) of each cell line was added to a centrifuge tube and mixed by pipetting prior to plating in dishes together. Cells were allowed to grow at 37 °C with 5% CO_2 for 72-96 h. All media was removed from the dishes, and cells were washed once with 1 mL PBS. 150 µL of 0.8 nM phage in flow cytometry buffer (see above) was added to each well of the plate, and the dishes were returned to an incubator at 37 °C with 5% CO_2. After 1 h, 1 mL room temperature flow cytometry buffer was added to gently wash the cells and removed; 2 more washes with 1 mL r.t. flow cytometry buffer were performed, and then 1 mL phenol red-free media (with FBS) was added to the cells. DAPI was added at 1 µM prior to imaging. Images were acquired on a Zeiss 510 NLO Axiovert 200M Tsunami microscope equipped with 488 and 633 nm lasers.

7. Preparation of xenograft models. All tumor xenografts were prepared in the Preclinical Therapeutics Core Facility at UCSF using IACUC- and ACURO-approved protocols. Tumor cells for injection are cultured under sterile conditions according to ATCC recommended guidelines. For HCC1954 cells (subcutaneous xenograft), tumor cells were harvested, and 5 million cells injected into each anesthetized mouse (5 total) in a 150 µL single cell suspension in a 1:1 mixture of growth media with the matrix additive Matrigel into the flank using individual sterile syringes and 25g 5/8 needles. For MDA-MB-231 cells (orthotopic implantation), tumor cells are harvested, and 8 million cells per mouse injected into surgically exposed number 4 mammary fat pads with a 100 µL Hamilton syringe.

8. Optical imaging. All imaging experiments were conducted at the Center for Molecular and Functional Imaging at UCSF using IACUC- and ACURO-approved protocols. Optical imaging was performed using an IVIS 50 (Caliper Life Sciences) instrument. Prior to injection with imaging agents, animals were anesthetized with isoflurane, and pre-injection images acquired. 2 nmol of each agent (based on dye concentration) in 150 µL PBS was injected via tail vein. Images were acquired at the following time points: 10 min, 30 min, 1 h, 2 h, 3 h, 4 h, 5 h, 6 h, 7 h, 8 h, 24 h, 48 h, and 72 h (except where euthanasia preceded that acquisition). The first assay with a particular agent continued until it had cleared in order to determine optimal time points for *ex vivo* biodistribution.

KEY RESEARCH ACCOMPLISHMENTS:

1. Generation of phage targeting epidermal growth factor receptor (EGFR), human epidermal growth factor receptor 2 (HER2), and botulinum toxin type A (BoNT/A; control) via infection and growth in *e. coli*.

2. Successful modification of anti-EGFR, -HER2 and –BoNT/A phage pVIII coat proteins via pyridoxal 5‟-phosphate (PLP) mediated transaminations followed by appendage of fluorophores and polyethylene glycol (PEG) chains at various levels.

3. Confirmation of binding abilities of modified anti-EGFR, -HER2, and –BoNT/A (control) phage in breast cancer and other cell lines (A431, HCC1954, Jurkat, L3.6pl, M6, M6c, MCF-7, MCF-7 clone 18, MDA-MB-231, MDA-MB-453, SKBR3, SUM52-PE, U87MG) possessing varying levels of expression of the respective proteins by using flow cytometry.

4. Visualization of modified anti-EGFR and anti-HER2 phage binding to live HCC1954, MDA-MB-231, and MCF7 clone 18 breast cancer cell lines.

5. Established subcutaneous tumors using HCC1954 cells, and performed optical imaging experiments with anti-HER2 and anti-BoNT/A (control) phage.

6. Established orthotopic tumors using MDA-MB-231 cells in mouse mammary fat pads. Performed optical imaging experiments with anti-EGFR (with and without PEG modification) and anti-BoNT/A (control) phage.

REPORTABLE OUTCOMES: Provide a list of reportable outcomes that have resulted from this research to include:

Manuscript in preparation:

1. Carrico, Z. M.; Farkas, M. E.; Hsiao, S. C.; Chokhawala, H.; Clark, D. S.; Marks, J. D.; Francis, M. B. **“**Chemically customizable filamentous phage” (2011)

Poster presentations:

1. Farkas. M. E.; Carrico, Z. M.; Tong, G. J.; Wu, W.; Behrens, C. R.; Gray, J. M.; Francis, M. B. “Chemically Modified Bacteriophage as a Streamlined Approach Toward Non-Invasive Breast Cancer Imaging” **Gordon Conference in Mammary Gland Biology**, Newport, RI, June 2011

2. Farkas. M. E.; Carrico, Z. M.; Tong, G. J.; Wu, W.; Behrens, C. R.; Gray, J. M.; Francis, M. B. “Chemically Modified Bacteriophage as a Streamlined Approach Toward Non-Invasive Breast Cancer Imaging” **Department of Defense Breast Cancer Research Program 6th Era of Hope Conference**, Orlando, FL, August 2011

CONCLUSION: During the first year of research I have successfully generated and selectively modified filamentous phage targeting HER2 and EGFR, and the control phage, anti-BoNT/A, to display various levels of fluorophores and PEG chains. These agents have been demonstrated to specifically bind to a panel of cell lines possessing varying levels of HER2 and EGFR receptors *in vitro* via flow cytometry and confocal microscopy assays. Having developed robust growth and reaction conditions, and confirmed the binding abilities of the modified fd, the panel of agents to be evaluated will be expanded to include phage targeting CD44, HER3, and CD73 cancer markers. Initial phage imaging experiments have been conducted with two types of xenograft models (HCC1954 and MDA-MB-231). Both assays have provided significant preliminary information with regard to biodistribution and tumor targeting capabilities of the agents, however, tumor cell lines and sites are being evaluated in order to determine optimal imaging conditions. In the event that the phage are unable to target tumors of interest selectively in animal models, we plan to evaluate other scaffolds and will look into *in vivo* phage display methods in order to produce agents with improved targeting capabilities. The current results have demonstrated we can directly modify filamentous phage via chemical methods and retain their binding capabilities. Furthermore, we have shown that the phage are able to clear from the animals in a time-frame suitable for imaging agents. Even if these particular fd are not found to bind tumors *in vivo*, the methodology developed can be used to generate imaging agents for other library-identified targeted phage.

REFERENCES:

1. Arap, W.; Haedicke, W.; Bernasconi, M.; Kain, R.; Rajotte, D.; Krajewski, S.; Ellerby, H. M.; Bredesen, D. E.; Pasqualini, R.; Ruoslahti, E. Targeting the prostate for destruction through a vascular address. *Proc. Natl. Acad. Sci. U. S. A.* **2002**. *99,* 1527-1531.
2. Newton-Northup, J. R.; Figueroa, S. D.; Quinn, T. P.; Deutscher, S. L. Bifunctional phage-based pretargeted imaging of human prostate carcinoma. *Nucl. Med. Biol.* **2009**. *36,* 789-800.
3. Kelly, K. A.; Waterman, P.; Weissleder, R. In vivo imaging of molecularly targeted phage. *Neoplasia.* **2006**. *8,* 1011-1018.
4. Yacoby, I.; Benhar, I. Targeted filamentous bacteriophages as therapeutic agents. *Expert Opin. Drug Deliv.* **2008**. *5,* 321-329.
5. Heitner, T.; Moor, A.; Garrison, J. L.; Marks, C.; Hasan, T.; Marks, J. D. Selection of cell binding and internalizing epidermal growth factor receptor antibodies from a phage display library. *J. Immunol. Methods.* **2001**. *248,* 17-30.
6. Poul, M. A.; Becerril, B.; Nielsen, U. B.; Morisson, P.; Marks, J. D. Selection of tumor-specific internalizing human antibodies from phage libraries. *J. Mol. Biol.* **2000**. *301,* 1149-1161.
7. Amersdorfer, P.; Marks, J. D. Phage libraries for generation of Anti-Botulinum scFv antibodies. *Methods Mol. Biol.* **2000**. *145,* 219-240.
8. Chiu, C. G.; Masoudi, H.; Leung, S.; Voduc, D. K.; Gilks, B.; Huntsman, D. G.; Wiseman, S.M. HER-3 Overexpression is prognostic of reduced breast cancer survival: a study of 4046 patients. *Ann. Surg.* **2010**. *251,* 1107-1116.
9. Lopez, J. I.; Camenisch, T. D.; Stevens, M. V.; Sands, B. J.; McDonald, J.; Schroeder, J. A.; CD44 attenuates metastatic invasion during breast cancer progression. *Cancer Res.* **2005.** *65*, 6755-6763.
10. Fillmore, C.; Kuperwasser, C. Human breast cancer stem cell markers CD44 and CD24: enriching for cells with functional properties in mice or in man? *Breast Cancer Res.* **2007.** *9,* 303.
11. Zhi, X.; Wang, Y.; Zhou, X.; Yu, J.; Jian, R.; Tang, S.; Yin, L.; Zhou, P. RNAi-mediated CD73 suppression induces apoptosis and cell-cycle arrest in human breast cancer cells. *Cancer Sci.* **2010,** *101,* 2561-2569.
12. Stagg, J.; Divisekera, U.; McLaughlin, N.; Sharkey, J.; Pommey, S.; Denoyer, D.; Dwyer, K. M.; Smyth, M. J. Anti-CD73 antibody therapy inhibits breast tumor growth and metastasis. *Proc. Natl. Acad. Sci. U.S.A.,* **2010,** *107,* 1547-1552.
13. Zhou, Y.; Marks, J. D. Identification of target and function specific antibodies for effective drug delivery. *Therapeutic Antibodies: Methods and Protocols.* **2009**. *525,* 145-160.
14. Gilmore, J. M.; Scheck, R. A.; Esser-Kahn, A. P.; Joshi, N. S.; Francis, M. B. N-terminal protein modification through a biomimetic transamination reaction. *Angew. Chem.-Int. Edit.* **2006**. *45,* 5307-5311.
15. Scheck, R. A.; Francis, M. B. Regioselective labeling of antibodies through N-terminal transamination. *ACS Chem. Biol.* **2007**. *2,* 247-251.
16. Scheck, R. A.; Dedeo, M. T.; Lavarone, A. T.; Francis, M. B. Optimization of a biomimetic transamination reaction. *J. Am. Chem. Soc.* **2008**. *130,* 11762-11770.
17. Hooker, J. M.; Esser-Kahn, A. P.; Francis, M. B. Modification of aniline containing proteins using an oxidative coupling strategy. *J. Am. Chem. Soc.* **2006**. *128,* 15558-15559.
18. Carrico, Z. M.; Francis, M. B. *Unpublished Results,*
14. Roser, M.; Fischer, D.; Kissel, T. Surface-modified biodegradable albumin nano- and microspheres. II: effect of surface charges on in vitro phagocytosis and biodistribution in rats. *Eur. J. Pharm. Biopharm.* **1998**. *46,* 255-263.

Supporting information:

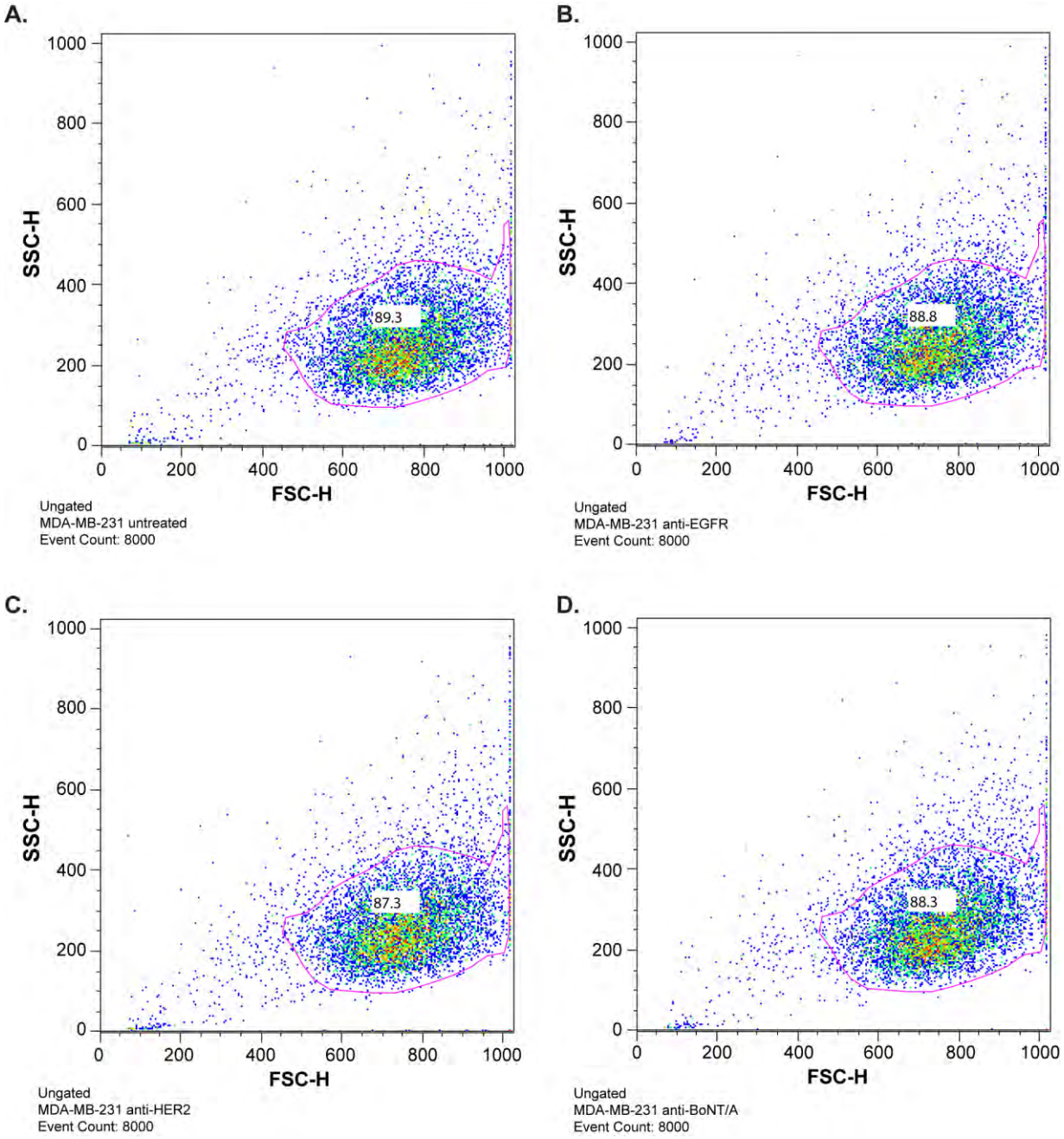

Figure S1. Forward and side scatter plots for flow cytometry with MDA-MB-231 cells. Plots are shown for (**a**) untreated, (**b**) anti-EGFR phage treated, (**c**) anti-HER2 phage treated, and (**d**) anti-BoNT/A treated cells. Gating used for histogram generation (**Figure 2a**) is indicated by the pink outline. Number inside of the plot reflects percentage of cells within each gate.

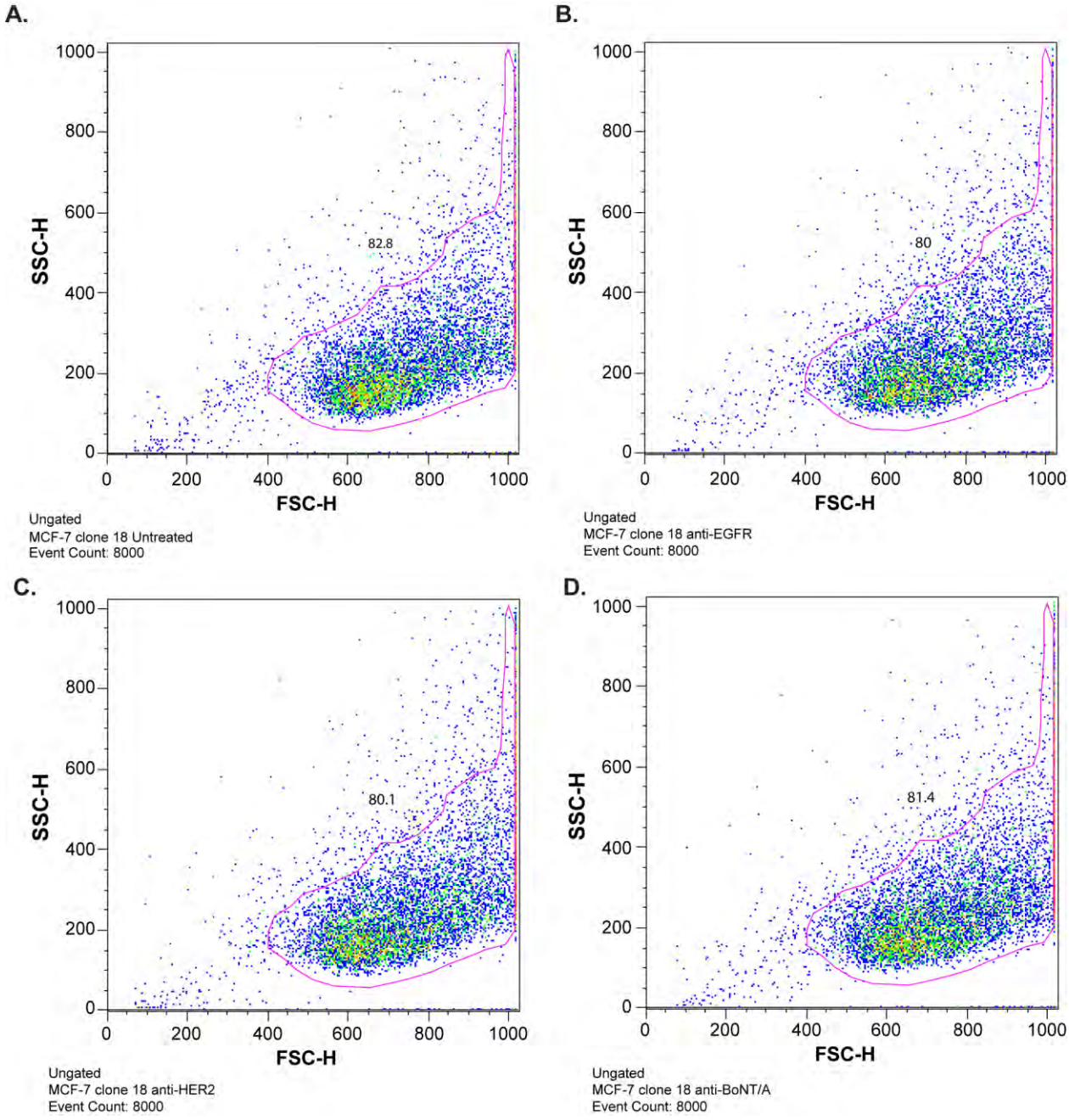

Figure S2. Forward and side scatter plots for flow cytometry with MCF-7 clone 18 cells. Plots are shown for (**a**) untreated, (**b**) anti-EGFR phage treated, (**c**) anti-HER2 phage treated, and (**d**) anti-BoNT/A treated cells. Gating used for histogram generation (**Figure 2b**) is indicated by the pink outline. Number inside of the plot reflects percentage of cells within each gate.

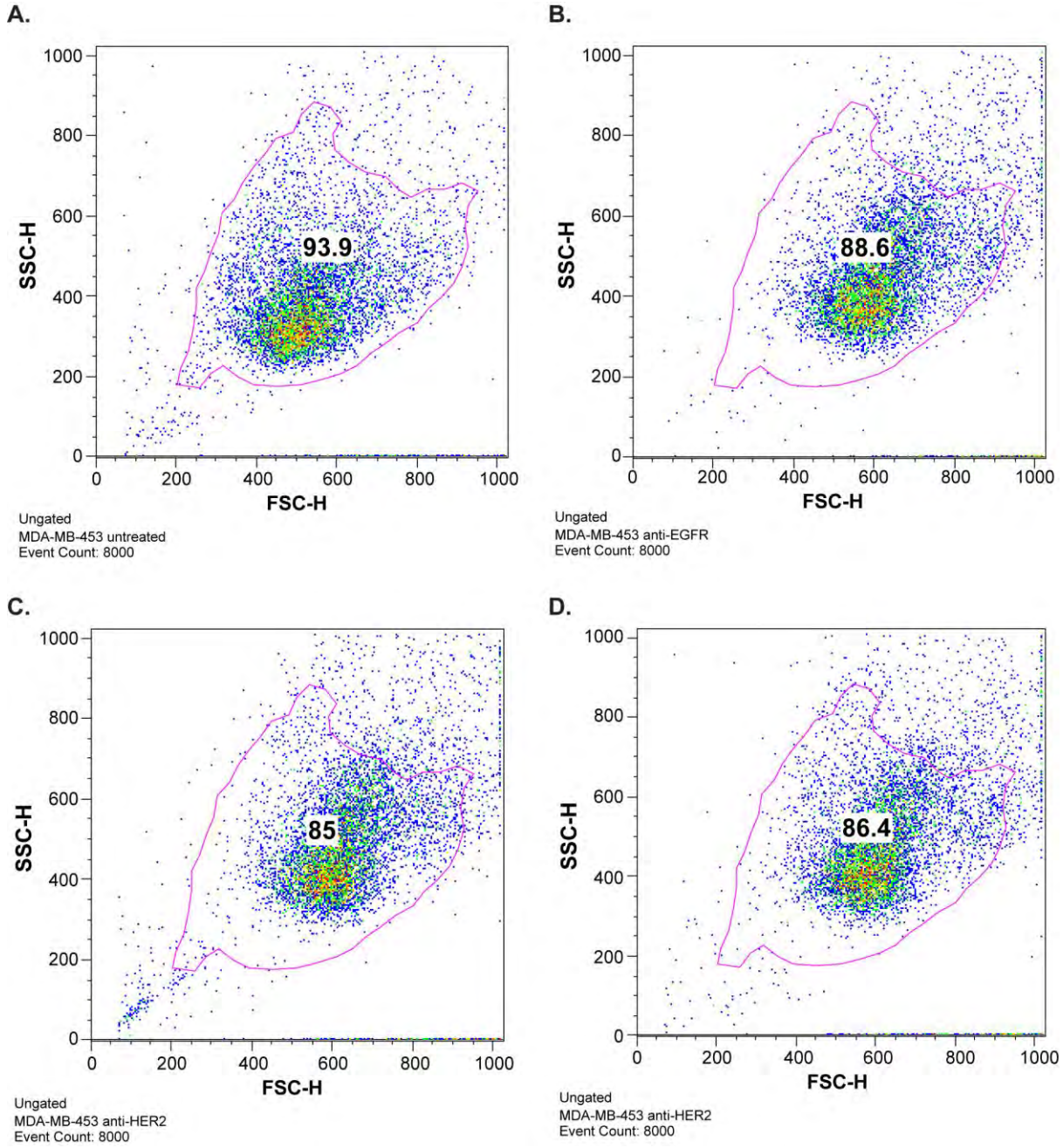

Figure S3. Forward and side scatter plots for flow cytometry with MDA-MB-453 cells. Plots are shown for (**a**) untreated, (**b**) anti-EGFR phage treated, (**c**) anti-HER2 phage treated, and (**d**) anti-BoNT/A treated cells. Gating used for histogram generation (**Figure 2c**) is indicated by the pink outline. Number inside of the plot reflects percentage of cells within each gate.

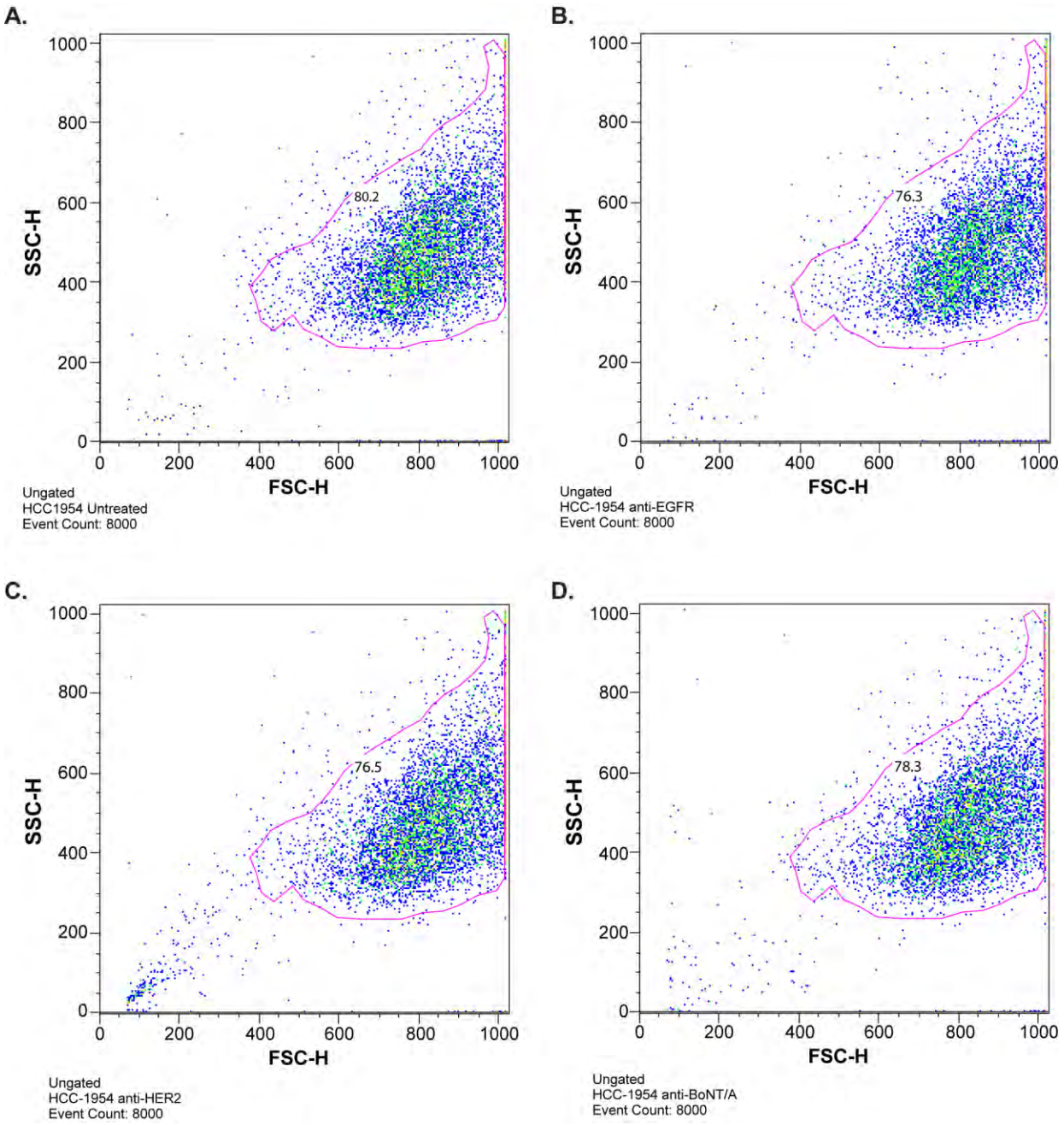

Figure S4. Forward and side scatter plots for flow cytometry with HCC1954 cells. Plots are shown for (**a**) untreated, (**b**) anti-EGFR phage treated, (**c**) anti-HER2 phage treated, and (**d**) anti-BoNT/A treated cells. Gating used for histogram generation (**Figure 2d**) is indicated by the pink outline. Number inside of the plot reflects percentage of cells within each gate.

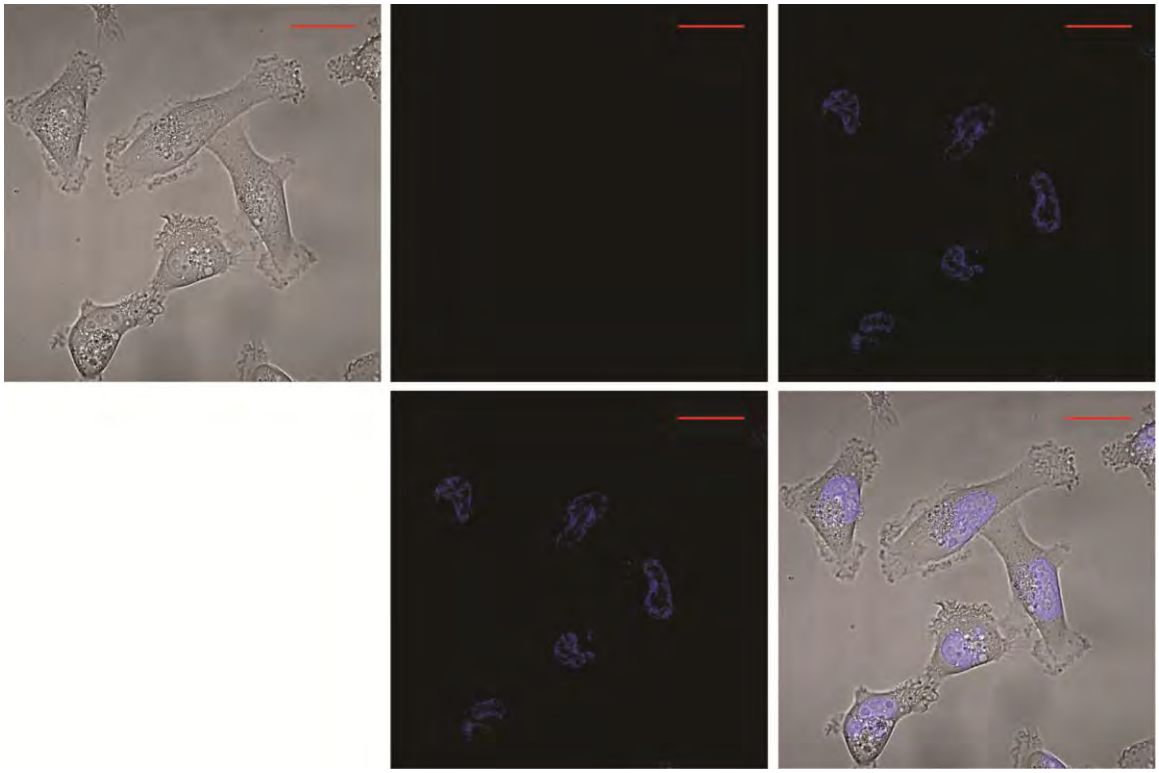

Figure S5. Live cell confocal microscopy images of MDA-MB-231 cells. Cells are treated with anti-HER2 phage (red), and DAPI (blue). Scale bars indicate 20 μm. Top row (L to R): bright-field image, red channel only, blue channel only; bottom row (L to R): all fluorescent channels, merge.

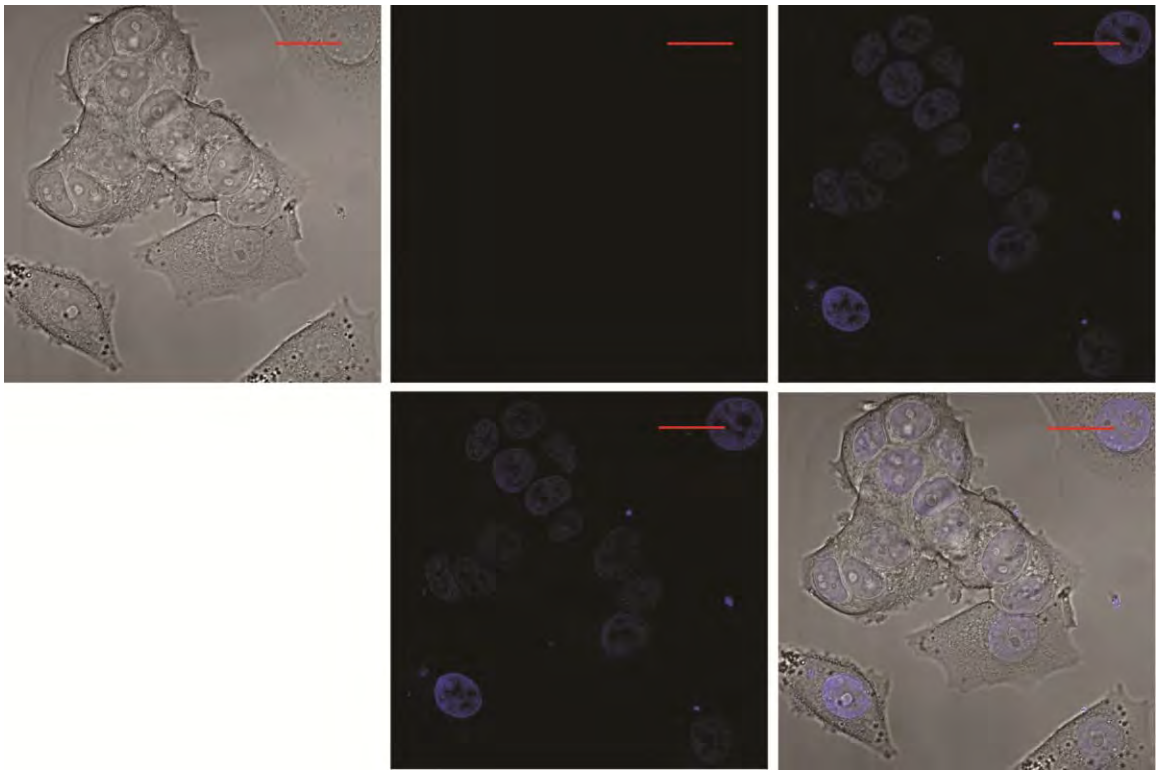

Figure S6. Live cell confocal microscopy images of MCF-7 clone 18 cells. Cells are treated with anti-EGFR phage (green), and DAPI (blue). Scale bars indicate 20 μm. Top row (L to R): bright-field image, green channel only, blue channel only; bottom row (L to R): all fluorescent channels, merge.

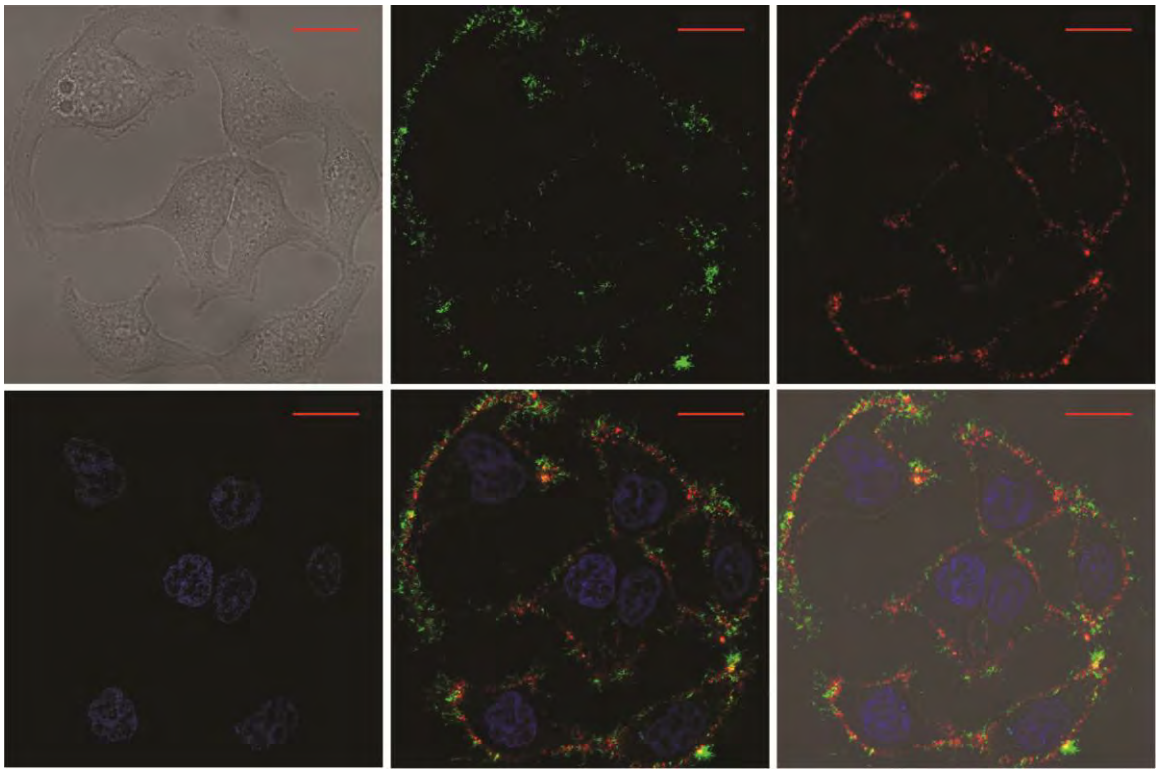

Figure S7. Live cell confocal microscopy images of HCC1954 cells. Cells are treated with anti-EGFR phage (green), anti-HER2 phage (red), and DAPI (blue). Scale bars indicate 20 μm. Top row (L to R): bright-field image, green channel only, red channel only; bottom row (L to R): blue channel only, all fluorescent channels, merge.

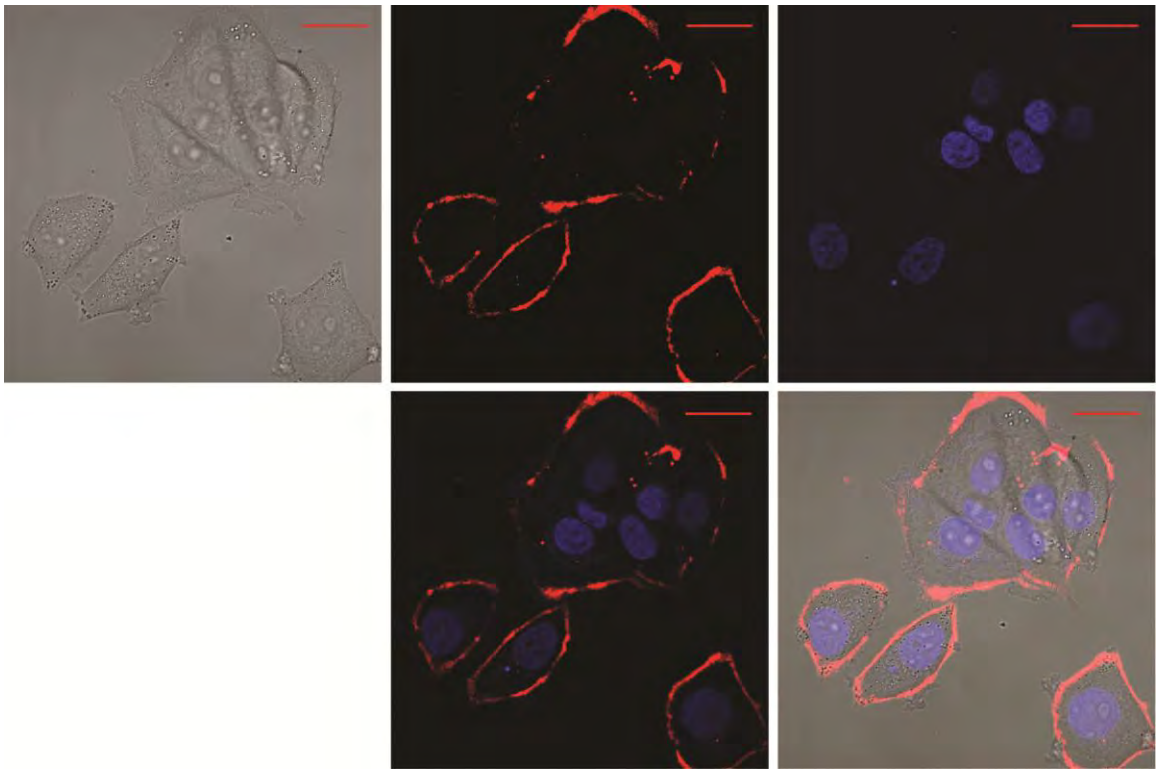

Figure S8. Live cell confocal microscopy images of MCF-7 clone 18 cells. Cells are treated with anti-HER2 phage (red), and DAPI (blue). Scale bars indicate 20 μm. Top row (L to R): bright-field image, red channel only, blue channel only; bottom row (L to R): all fluorescent channels, merge.

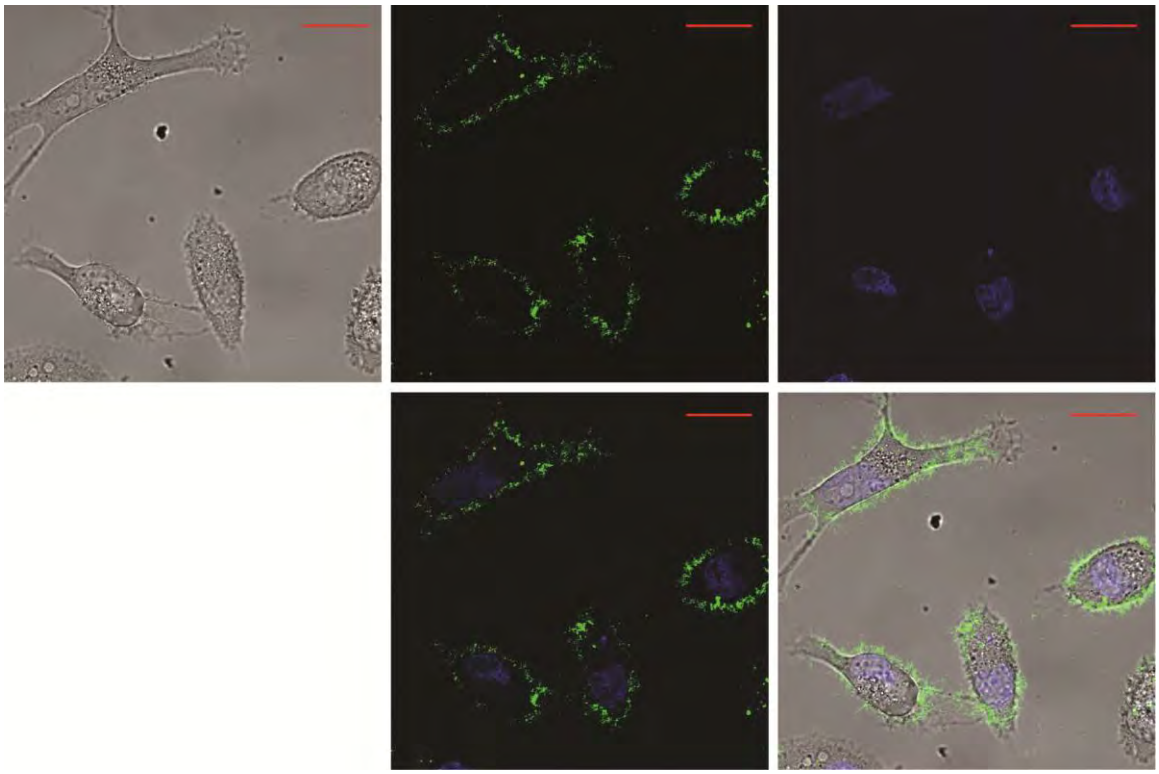

Figure S9. Live cell confocal microscopy images of MDA-MB-231 cells. Cells are treated with anti-EGFR phage (green), and DAPI (blue). Scale bars indicate 20 μm. Top row (L to R): bright-field image, green channel only, blue channel only; bottom row (L to R): all fluorescent channels, merge.

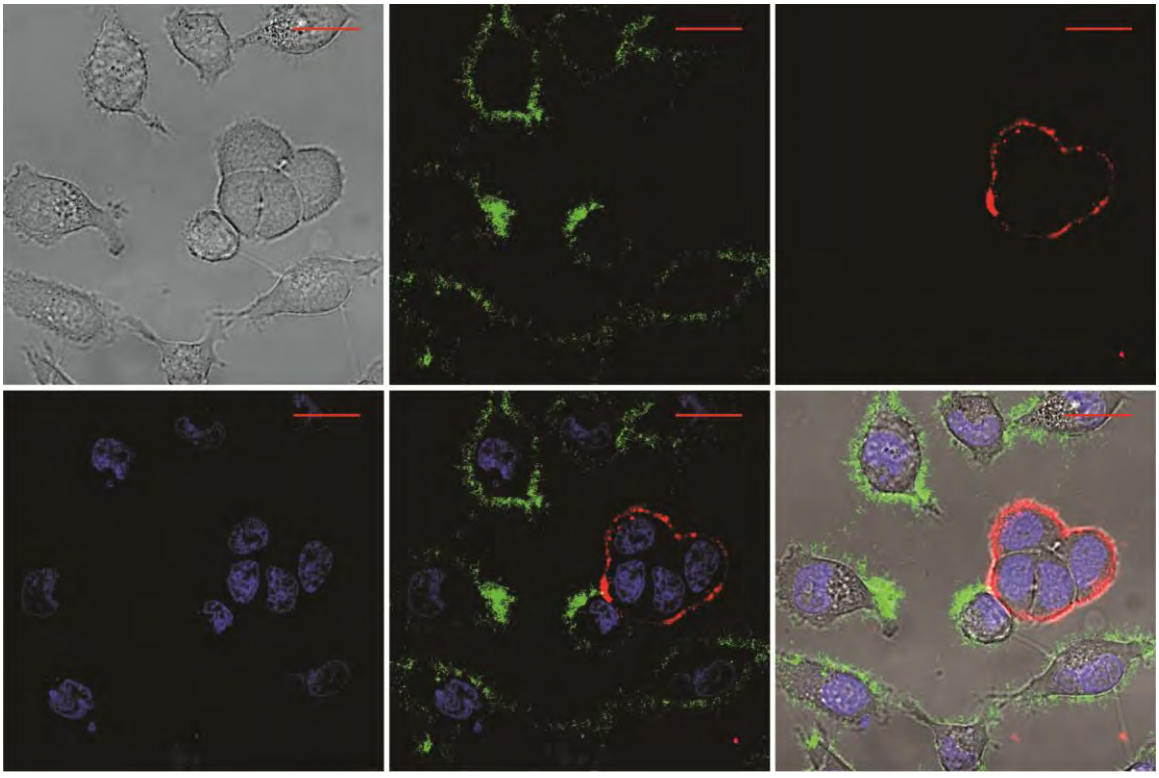

Figure S10. Live cell confocal microscopy images of co-cultured MDA-MB-231 and MCF-7 clone 18 cells. Cells are treated with anti-EGFR phage (green), anti-HER2 phage (red), and DAPI (blue). Scale bars indicate 20 μm. Top row (L to R): bright-field image, green channel only, red channel only; bottom row (L to R): blue channel only, all fluorescent channels, merge.